

Statistical ages and the cooling rate of X-ray dim isolated neutron stars

Ramandeep Gill^{1,2*} and Jeremy S. Heyl^{1†}

¹*Department of Physics and Astronomy, University of British Columbia, 6224 Agricultural Road, Vancouver, British Columbia, Canada V6T 1Z1*

²*Canadian Institute for Theoretical Astrophysics, University of Toronto, 60 St. George Street, Toronto, Ontario, M5S 3H8*

Accepted —. Received —; in original form —

ABSTRACT

The cooling theory of neutron stars is corroborated by its comparison with observations of thermally emitting isolated neutron stars and accreting neutron stars in binary systems. An important ingredient for such an analysis is the age of the object, which, typically, is obtained from the spin-down history. This age is highly uncertain if the object’s magnetic field varies appreciably over time. Other age estimators, such as supernova remnant ages and kinematic ages, only apply to few handful of neutron stars. We conduct a population synthesis study of the nearby isolated thermal emitters and obtain their ages statistically from the observed luminosity function of these objects. We argue that a more sensitive blind scan of the galactic disk with the upcoming space telescopes can help to constrain the ages to higher accuracy.

Key words: stars: magnetic fields - stars: neutron - magnetars

1 INTRODUCTION

The observed thermal states of isolated neutron stars have become the primary source to glean useful and interesting information about the internal structure of neutron stars (NSs). Reconciliation of theoretical cooling curves with observations of nearby isolated cooling NSs is a challenging task (see for e.g. Yakovlev & Pethick 2004; Page et al. 2006, for a comprehensive review). On the theoretical front, the problem arises from incomplete knowledge of the composition and equation of state (EOS) of matter in the NS core at supernuclear densities ($\rho > 10^{14} \text{gcm}^{-3}$). Many possibilities can be realized: Depending on the composition the EOS can be either *soft* or *stiff*, where the stiffness characterizes the compressibility of matter, and strongly depends on the internal degrees of freedom of the system (e.g. Schaab et al. 1996). For example, for a polytropic EOS, $P = K\rho^\Gamma$, a larger adiabatic index Γ yields stiffer EOS. Such an EOS generally produces larger maximum masses and radii of NSs than its softer counterpart. Softer EOSs can be obtained by the introduction of phase transitions in the theory where the core of the NS may be composed of boson condensates, quark or hyperonic matter. However, the presence of these at nuclear densities has been ruled out from the observation of a $1.97 \pm 0.04 M_\odot$ NS (Demorest et al. 2010). The cooling behavior of NSs depends very sensitively on the composition of

the inner core, such that it affects the choice of the neutrino cooling process that is dominant in the first $10^4 - 10^5$ yrs of its evolution (see for e.g. Yakovlev et al. 2001, for a detailed description of all the neutrino emission processes in NSs).

X-ray observations of isolated cooling NSs have been crucial in their discovery (see for e.g. Mereghetti 2011). However, these observations present its own set of challenges in determining their cooling rate. Here, one is interested in detecting radiation emanating from the surface of the NS which, in the case of pulsars, is complicated by the non-thermal emission from the magnetosphere. Also, the non-uniform heating of the crust due to energetic particles accelerated in the magnetosphere render accurate determination of effective temperatures hard (see for e.g. the review by Özel 2013, on surface emission from NSs). The unknown composition of NS atmospheres leads to the overestimation of their temperatures when fitting their spectra with a blackbody (e.g. Lloyd et al. 2003). Apart from the uncertainties involved in the spectral modelling of NS surface emission, uncertainties in their distances can also contribute to poor effective temperature and luminosity estimates. Furthermore, to place observed isolated sources on cooling curves, accurate ages are needed that may be hard to obtain as we discuss below.

In this study, we show that, for a large sample, ages of isolated thermal emitters can be derived from statistical arguments. As the sample size grows, the statistical error diminishes. We look at a small group of thermally emitting NSs discovered in the ROSAT all-sky survey in Sec. 2 and

* E-mail: rgill@cita.utoronto.ca

† E-mail: hey1@phas.ubc.ca; Canada Research Chair

derive their ages statistically in Sec. 3. Lastly, we discuss the possibility of improving the meager sample of isolated thermal emitters by detecting more such objects in the upcoming eROSITA all-sky survey.

2 THE MAGNIFICENT SEVEN

Nearby isolated cooling neutron stars are particularly important for confronting cooling models with observations. They were discovered by Einstein, ROSAT, and ASCA space telescopes (Becker & Pavlov 2002), and were further observed with the extremely sensitive and high resolution high-energy space telescopes Chandra and XMM-Newton. Among all the discovered objects, the most interesting are the seven radio-quiet thermally emitting isolated NSs (a.k.a. the magnificent seven, M7) discovered in the ROSAT all-sky survey (RASS) (see for e.g. Haberl 2007, for a review). These radio-quiet objects radiate predominantly in X-rays with high X-ray to optical flux ratios, $f_X/f_{opt} > 10^{4-5}$. Their soft X-ray spectra are reasonably well fit by an absorbed blackbody-like spectrum with $kT \lesssim 100$ eV and a hydrogen column density $n_H \sim 10^{20}$ cm $^{-2}$, indicating small distances $d \sim \text{few} \times 100$ pc. Astrometric measurements of some of the member objects independently confirm the distances inferred from column densities (see references in Table 2). That the thermal emission is coming from majority of the stellar surface is confirmed by the small pulse fractions $\lesssim 20\%$ of the X-ray light curves. Spin periods ranging from 3 - 12 s have been measured for all but one (RX J1605.3+3249) of the M7 objects (see for e.g. Mereghetti 2011, Table 2). This in conjunction with the measured spin-down rates, $\dot{P} \sim 10^{-14} - 10^{-13}$ s s $^{-1}$, yields an estimate of the polar magnetic field strengths $B_p \sim 10^{13}$ G and the characteristic spin-down ages $\tau_c \sim 10^6$ years (Kaplan & van Kerkwijk 2005a,b, 2009a,b, 2011; van Kerkwijk & Kaplan 2008). Measurements of the high proper motions of three of the M7 objects and their association thus established to the Sco OB2 complex comprising the Gould Belt yield kinematic and/or dynamical ages that are smaller than ages inferred from spin down (Kaplan et al. 2002, 2007; Walter & Lattimer 2002; Motch et al. 2005, 2009; Tetzlaff et al. 2010, 2011; Mignani et al. 2013).

The discrepancy between characteristic and kinematic ages strongly suggests that the spin-down ages are overestimates and the M7 objects in reality are much younger (see for e.g. Kaplan & van Kerkwijk 2005a, 2009a). Even when considering simple cooling models (Heyl & Hernquist 1998; Pons et al. 2009), one finds the spin-down ages to be 3 - 4 times in excess of the cooling ages of ~ 0.5 Myr (Kaplan et al. 2002).

2.1 Spin-Down Ages: Poor Age Estimators

According to the standard magnetic dipole model of pulsars (Shapiro & Teukolsky 1983), a rotating NS with a polar magnetic field spins down over time by emitting magnetic dipole radiation. From the rate of change of the angular frequency $\dot{\Omega}$, the spin-down age of the NS can be readily determined, with the assumption that the initial angular frequency is much larger than the present value ($\Omega_0 \gg \Omega(t)$),

$$\tau = \frac{\Omega}{2|\dot{\Omega}|} \quad (1)$$

This assumption is invalid in the case of CCOs as these objects are believed to have their initial periods very close to the current values (e.g. Halpern & Gotthelf 2010a). The spin-down law implicitly assumes that none of the other physical characteristics of the pulsar vary over time. This may not be the case and, in general, the spin-down law (Lyne & Graham-Smith 2006) written as the following can be allowed to include variation of B_p , the moment of inertia I , and the angle between the rotation axis and the magnetic dipole axis α , so that

$$\frac{d\Omega}{dt} = -\kappa(t)\Omega(t)^n \quad (2)$$

where $\kappa(t)$ is usually assumed to be a constant and $n = 3$ is the *braking index* for magnetic dipole braking. Any change in κ with time naturally yields ages of pulsars that are in conflict with their spin-down ages; Generally, the spin-down age should only be taken as a rough estimate to aid in calculations.

An independent age estimate is provided by the age of the associated supernova remnant (SNR) or massive star cluster for younger objects. Establishing such an association for older NSs may prove to be difficult since SNRs fade away in ~ 60 kyr, and in the same time, due to natal kicks (~ 500 km s $^{-1}$), NSs may move significantly far away from their birth sites (Frail et al. 1994). We plot the spin-down and the estimated SNR ages for young pulsars ($\tau < 10^5$ yrs), central compact objects (CCOs), and magnetars (SGRs and AXPs) along with their timing properties (see for e.g. Becker 2009, for a review) in Fig. 1, and it is clear that for many NSs, that are not the typical spin-down powered radio pulsars, the characteristic age is a poor age estimator. The objects that have SNR ages smaller than their spin-down ages can be explained by having a braking index less than the *canonical* value, $n < 3$. An excellent example supporting this notion is the Vela pulsar which has a very small braking index $n = 1.4 \pm 0.2$ estimated from an impressive 25-year long observation (Lyne et al. 1996), albeit under the assumption that κ is still a constant. This yields a spin-down age of 25.6 kyr, making it appear more than twice as old as its age inferred from the standard magnetic braking scenario. This result is well supported by the estimated age of the Vela SNR ($t_{\text{SNR}} \sim 18 - 31$ kyr) (Aschenbach et al. 1995).

On the other hand, for objects that have spin-down ages larger than that of their true ages, that may be inferred from their associated SNR ages, it can be argued that the magnetic moments decrease in strength over time (Heyl & Kulkarni 1998). There are three main mechanisms by which magnetic fields can decay in isolated NS, namely Ohmic dissipation, ambipolar diffusion, and Hall drift (Goldreich & Reisenegger 1992). The timescale over which the field decays substantially due to these processes (see for e.g. Heyl & Kulkarni 1998) determines the dominating process at different stages in the evolution of an isolated NS.

An important consequence of field decay is that it leads to an overestimation of the real age of the NS. Following the analysis of (Colpi et al. 2000, see Eq. 2, 3, and 4), we plot in Fig. 1 the change in the spin-down age of the object over

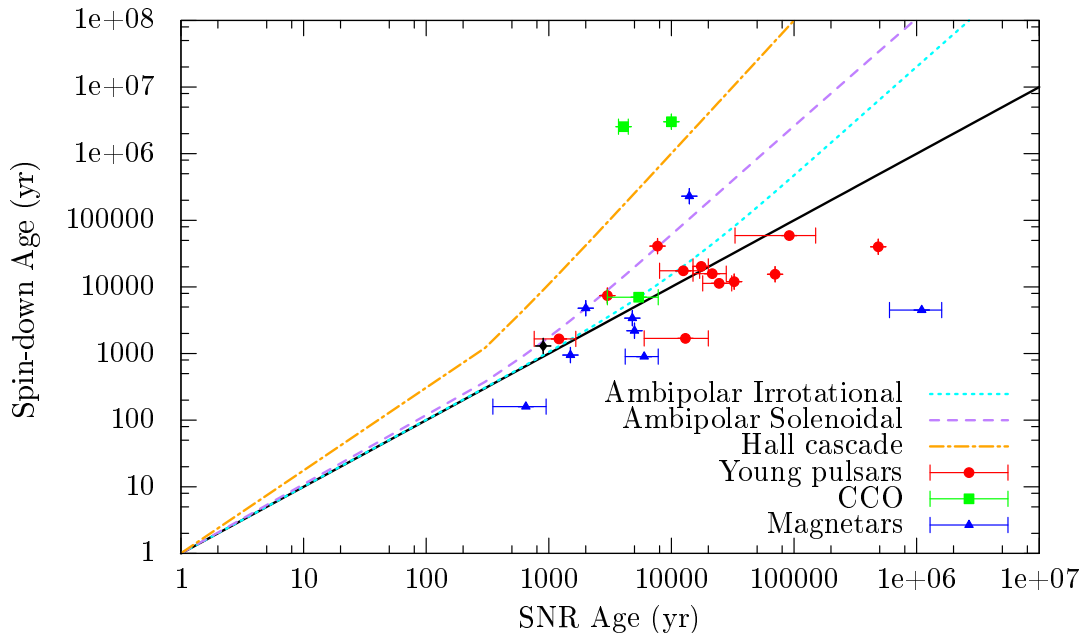


Figure 1. Change in the spin-down or characteristic age of an isolated NS due to various magnetic field decay mechanisms, namely the ambipolar (I)rrotational ($a = 0.01$, $\alpha = 5/4$, dotted) and (S)olenoidal ($a = 0.15$, $\alpha = 5/4$, dashed) modes, and the Hall cascade ($a = 10$, $\alpha = 1$, dot-dashed) (See Eq. 2 - 4 of Colpi et al. 2000). The solid black line denotes $t = \tau$, meaning no field decay. This assumes an initial field strength $B_0 = 10^{16}$ G and period $P_0 = 1$ ms. The Crab pulsar is shown here with a black diamond.

time due to the decaying strength of the magnetic field by the aforementioned processes.

$$\tau(t) = \frac{P(t)^2}{2bB(t)^2} \quad (3)$$

where $b \approx 10^{-39}$ in cgs units. The effect of field decay at late times is apparent from the divergence of the characteristic age from the real age.

3 TRUE AGE ESTIMATES OF ISOLATED NEUTRON STARS

The M7 objects don't have any SNR or massive star cluster associations. Therefore, ages for these objects have been derived from their P and \dot{P} measurements. In addition, since they are nearby objects ($d \lesssim 500$ pc), and due to their large proper motions, kinematic ages became a possibility and have been estimated for only four of the group members (see Table 2). In this case, one finds that the spin-down ages are larger by a factor of 3–10 than the kinematic ages. Accurate age estimates are extremely important in determining the cooling behavior of isolated NSs. Overestimated ages used to fit model cooling curves can obscure the determination of the true thermal state of these objects.

3.1 Age Estimates from Population Synthesis

In the following, we estimate the true ages of the M7 members by a method that is motivated by another method devised by Schmidt (1968) and then applied by Huchra & Sargent (1973) to calculate the luminosity function of field galaxies. The original idea is implemented as

follows. An apparent magnitude limited sample is first obtained and it is assumed that the objects in the sample, field galaxies for instance, are distributed uniformly in Euclidean space, such that the luminosity function is independent of the distance. Then, to each object an *accessible volume* $V_{\max}(M)$ is assigned (Avni & Bahcall 1980). This volume depends on the absolute magnitude of the object and gives a measure of the volume surveyed for a given object with an absolute magnitude M . Basically, $V_{\max}(M)$ is the maximum volume in which the object would be detected had its apparent magnitude been equal to the limiting magnitude of the survey. The whole sample is then divided into bins of size dM with objects having absolute magnitude in the range $[M - dM/2, M + dM/2]$. The luminosity function for this bin is estimated by adding the inverse of the accessible volumes for each object in that bin

$$\Phi(M) (\text{Mpc}^{-3} \text{mag}^{-1}) = \sum_i \frac{1}{V_{i,\max}(M)}. \quad (4)$$

This method provides a non-parametric way of estimating the luminosity function and it exactly reproduces the true luminosity function within statistical errors (Hartwick & Schade 1990). Furthermore, this is a very general method which relies on only one underlying assumption that the objects are distributed according to their intrinsic brightnesses.

In the case of neutron stars (unlike galaxies) it is reasonable to assume that the birthrate has been constant over the past few million years, and furthermore, the neutron stars progress from bright to faint luminosities as they age in the same (albeit unknown) way. Under these assumptions we can deduce the age of a neutron star of a given absolute magnitude

Table 1. Properties of isolated NSs with SNR or massive star cluster associations

Object	P (s)	\dot{P} (10^{-15} s s $^{-1}$)	t_{sd} (kyr)	t_{snr} (kyr)	SNR/Cluster	References
Young Pulsars [†]						
0531+21	0.033	421	1.3	0.90	Crab Nebula	1, 2
1509-58	0.150	1536	1.691	6 – 20	MSH 15-52	3, 4, 5, 6, 7
0833-45	0.089	125	11.3	18 – 31	Vela XYZ	8, 24, 10
1853+01	0.267	208	20.3	15 – 20	W44	11, 12
0540-69	0.050	479	1.66	0.76 – 1.66	SNR 0540-693	13, 14
1610-50	0.232	495	7.4	~ 3.0	Kes 32	15, 16
1338-62	0.193	253	12	~ 32.5	G308.8-0.1	17, 18
1757-24	0.125	128	15.5	~ 70	G5.4-1.2	17, 19, 20
1800-21	0.134	134	15.8	15 – 28	W30	21, 22, 23
1706-44	0.102	93	17.5	8 – 17	G343.1-2.3	15, 24
1930+22	0.144	57.6	40	~ 486	G57.1+1.7	25, 19, 26
2334+61	0.495	193	41	7.7	G114.3+0.3	27, 22, 28
1758-23	0.416	113	59	33 – 150	W28	17, 22, 29
CCOs						
RX J0822.0-4300	0.122	0.00928 ± 0.00036	2.54×10^3	3.7 – 4.45	Puppis A	30, 31, 32
1E 1207.4-5209	0.424	0.02224 ± 0.00016	3.02×10^3	~ 10	G296.5+10.0	30, 33
CXOU J185238.6	0.105	0.00868 ± 0.00009	7	3 – 7.8	Kes 79	34, 35
Magnetars ^{††}						
CXOU J164710.2	10.6	< 400	> 420	$(4 \pm 1) \times 10^3$	Westerlund 1*	36, 37
CXOU J171405.7	3.83	6.4×10^4	0.95	~ 1.5	CTB 37B	38, 39
1E 1841-045	11.78	3.93×10^4	4.8	~ 2	Kes 73	40, 41
1E 2259+586	6.98	484	230	14	CTB 109	42, 43
1E 1048.1-5937	6.46	2.25×10^4	4.5	$(1.1 \pm 0.5) \times 10^3$	GSH 288.3-0.5-2.8	44, 45
SGR 0526-66	8.05	3.8×10^4	3.4	~ 4.8	N49	46, 47
SGR 1627-41	2.59	1.9×10^4	2.2	~ 5	G337.0-0.1	48, 49, 50
SGR 1900+14	5.2	9.2×10^4	0.90	$> 6 \pm 1.8$	Massive star cluster	51, 52
SGR 1806-20	7.6	7.5×10^5	0.16	$> 0.65 \pm 0.3$	Massive star cluster	53, 52

[†] <http://www.atnf.csiro.au/research/pulsar/psrcat> (Manchester et al. (2005)); ^{††} <http://www.physics.mcgill.ca/~pulsar/magnetar/main.html>;

* Westerlund 1 is a massive star cluster; (1) Hester (2008) and references therein; (2) Nugent (1998); (3) Seward & Harnden (1982); (4) Manchester et al. (1982); (5) Weisskopf et al. (1983); (6) Kaspi et al. (1994); (7) Seward et al. (1983); (8) Large et al. (1968); (24) Dodson et al. (2002); (10) Aschenbach et al. (1995); (11) Wolszczan et al. (1991); (12) Dermer & Powale (2013); (13) Seward et al. (1984); (14) Park et al. (2010); (15) Johnston et al. (1992); (16) Vink (2004); (17) Manchester et al. (1985); (18) Caswell et al. (1992); (19) Hobbs et al. (2004); (20) Blazek et al. (2006); (21) Clifton & Lyne (1986); (22) Yuan et al. (2010); (23) Finley & Oegelman (1994); (24) Dodson et al. (2002); (25) Hulse & Taylor (1975); (26) Kovalenko (1989); (27) Dewey et al. (1985); (28) Yar-Uyaniker et al. (2004); (29) Sawada & Koyama (2012); (30) Gotthelf et al. (2013); (31) Winkler & Kirshner (1985); (32) Becker et al. (2012); (33) Vasisht et al. (1997); (34) Halpern & Gotthelf (2010a); (35) Sun et al. (2004); (36) An et al. (2013); (37) Muno et al. (2006); (38) Sato et al. (2010); (39) Halpern & Gotthelf (2010b); (40) Dib et al. (2008); (41) Vasisht & Gotthelf (1997); (42) Gavriil & Kaspi (2002); (43) Sasaki et al. (2013); (44) Dib et al. (2009); (45) Gaensler et al. (2005); (46) Tiengo et al. (2009); (47) Park et al. (2012); (48) Esposito et al. (2009); (49) Esposito et al. (2009); (50) Corbel et al. (1999); (51) Mereghetti et al. (2006); (52) Tendulkar et al. (2012); (53) Nakagawa et al. (2009);

$$t(M) = \frac{1}{\beta} \int_{-\infty}^M \Phi(M') dM' \quad (5)$$

where β is the neutron-star birthrate per volume.

3.2 RASS and Population Synthesis

In the following, we develop a slight variant of the Schmidt (1968) estimator to calculate the true ages of the members of the M7 family. The method we develop cannot be completely model independent as the distribution of NSs in space, unlike that of galaxies over large scales, is not uniform. Since the progenitors of NSs mainly reside in the arms of a spiral galaxy, and for a natal kick velocity of, say ~ 500 km s $^{-1}$,

the NSs only travel a distance of ~ 50 pc from their birth sites within $\sim 10^5$ years. This is small compared to the scale height of the thin disk ~ 300 pc (Binney & Merrifield 1998). As a result, the Schmidt (1968) estimator cannot be used here. Instead, we look at the NS progenitor population and calculate the weight, that is used to determine the statistical age (see Eq. 6), for each M7 member by counting the number of massive OB stars that are found in the accessible volume V_{max} for that object. The population synthesis method is given in our earlier study (Gill & Heyl 2007), and essentially requires the assumption of the luminosity function and spatial distribution of massive OB stars in the galaxy (Bahcall & Soneira 1980), and the distribution of HI,

which we model as a smooth exponential disk both radially and vertically (Foster & Routledge 2003). As pointed out in Posselt et al. (2007), local clumpiness of the ISM will affect the level of absorption. Thus, distances derived from assuming a homogeneous model will also be affected. This presents a very small degree of uncertainty in V_{\max} , that is insignificant compared to other uncertainties in the model, e.g. the uncertainty in the SN rate used to derive statistical ages (see below).

All M7 objects were discovered by ROSAT which scanned the whole sky with a limiting count rate of 0.015 cts s^{-1} in the energy range $\sim 0.12 - 2.4 \text{ keV}$ (see Hünsch et al. 1999, for more details). The complete survey covers 92% of the sky for a count rate of 0.1 cts s^{-1} (Voges et al. 1999) and has yielded the most complete and sensitive survey of the soft X-ray sky. Therefore, it provides a perfect flux-limited sample for our study. Next, we calculate the weights for each object in the sample by simulating the RASS and finding the total number of massive OB stars in the volume V_{\max} , such that the statistically estimated age is given in terms of the typical age of their progenitors t_{OB} ,

$$t_{i,\text{stat}} \sim t_{\text{OB}} \sum_{j=1}^{j=i} \frac{N_j}{N_{j,\text{OB}}} \rightarrow t_{\text{OB}} \sum_{j=1}^{j=i} \frac{1}{N_{j,\text{OB}}} \quad (6)$$

where N_j is the number of M7 objects in a small absolute magnitude bin of size dM centered at M_j . Since the sample is of marginal size, $N_j = 1$ in this case. Then, $1/N_{j,\text{OB}}$ gives the number of massive OB stars per j^{th} object in the sample. We first calculate the number of OB stars that lie in the volume V_{\max} for each M7 member. Then, we rank the M7 objects with respect to their effective temperatures with the hottest member ranked first ($i = 1$) and the coolest ranked last ($i = 7$). According to Eq. 6, the weight for the first object is $N_{1,\text{OB}}^{-1}$, the second is $(N_{1,\text{OB}}^{-1} + N_{2,\text{OB}}^{-1})$, and so on.

The ages of NS progenitors are highly uncertain and are usually obtained by estimating the main sequence turn-off ages of the massive star cluster to which the NS may be associated (see for e.g. Smartt 2009, for a review). Typical ages of $\sim 3 - 15 \text{ Myr}$ have been estimated for the progenitors of NSs and magnetars. Figer et al. (2005) report the age of the cluster of massive stars, containing three Wolf-Rayet stars and a post main-sequence OB supergiant, associated to the magnetar SGR 1806–20 to be roughly $3.0 - 4.5 \text{ Myr}$. Also, Munro et al. (2006) report an age of $4 \pm 1 \text{ Myr}$ for the cluster Westerlund 1 which seems to be the birth site of another magnetar CXOU J164710.2 – 455216. In yet another study, Davies et al. (2009) find the age of the cluster associated to the magnetar SGR 1900 + 14 to be $14 \pm 1 \text{ Myr}$. Since the spin-down ages of magnetars are much smaller ($\sim 10^3 - 4 \text{ yr}$) than that of the clusters, the notion that the cluster age reflects the age of the progenitor, under the assumption of coevality of its members, is a valid one. In the case of SGR 1806–20 and CXOU J164710.2 – 455216, both groups find that the progenitor must be a massive star with $M > 40M_{\odot}$, except in the last study where the progenitor of SGR 1900 + 14 is claimed to be a lower mass star with initial MS mass of $17 \pm 2M_{\odot}$. Notwithstanding this last result, it has been claimed that magnetars may be the progeny of only sufficiently massive stars ($M \gtrsim 25M_{\odot}$) (Gaensler et al. 2005) that would, otherwise, have resulted in the formation of a black hole. Although the members of the M7 family

are endowed with fields an order of magnitude higher than the normal radio PSRs, they are not magnetars and can be argued to be the descendants of progenitors not much more massive than that of the normal radio PSRs. In that case, it is expected that the progenitor age t_{OB} will be considerably longer in comparison to that of magnetar progenitors. An upper limit on the ages of M7 progenitors can be placed from the age of the Gould Belt, $t_{\text{OB}} \leq t_{\text{GB}} \sim 30 - 60 \text{ Myr}$ (Torra et al. 2000).

From Eq. 6 the ages of the sample objects are proportional to t_{OB} , thus significant uncertainty in the progenitor age will yield erroneous ages. We estimate t_{OB} by considering the total number of OB stars in the Galaxy and the supernova rate corresponding to type Ib/c and type II supernovae,

$$t_{\text{OB}} \approx \frac{N_{\text{OB,Gal}}}{\beta_{\text{SN}}} \quad (7)$$

From our modeling of OB stars in the Galaxy (Gill & Heyl 2007), we estimate $N_{\text{OB,Gal}} \sim 5.2 \times 10^5$, and using the supernova (SN) rate reported by Diehl et al. (2006) $\beta_{\text{SN}} = 1.9 \pm 1.1 \text{ per century}$, we find $t_{\text{OB}} \approx 27 \pm 16 \text{ Myr}$.

Over the last few years, two new candidates have been added to the M7 group. The first object, 1RXS J141256.0 + 792204 dubbed *Calvera* (Rutledge et al. 2008), was actually cataloged in the RASS Bright Source Catalog (Voges et al. 1999) for having a high X-ray to optical flux ratio $F_X/F_V > 8700$. However, its large height above the Galactic plane ($z \approx 5.1 \text{ kpc}$), requiring a space velocity $v_z \gtrsim 5100 \text{ km s}^{-1}$, presents a challenge for its interpretation as an isolated cooling NS like the M7 members (see Rutledge et al. 2008, for a detailed discussion). Also, recent X-ray observations of *Calvera* done with the XMM-Newton space telescope found unambiguous evidence for pulsations with period $P = 59.2 \text{ ms}$ (Zane et al. 2011). The authors of this study argued that *Calvera* is most probably a CCO or a slightly recycled pulsar. The uncertainty in its nature (see Halpern 2011) doesn't warrant inclusion into our sample of radio-quiet isolated NSs. The second object 2XMM J104608.7 – 594306 (Pires et al. 2009), discovered serendipitously in an XMM-Newton pointed observation of the Carina Nebula hosting the binary system Eta Carinae, appears to be a promising candidate (see Table 2 for properties). This object was not detected in the RASS due to its larger distance ($\approx 2.3 \text{ kpc}$, based on its association to the Carina nebula) and higher neutral hydrogen absorption column density ($N_H = 3.5 \pm 1.1 \times 10^{21} \text{ cm}^{-2}$). Therefore, the accessible volume V_{\max} is the ROSAT surveyed volume plus the additional volume probed by the XMM-Newton's pointed observation.

In Table 2, we provide all the relevant data on the sample objects including the spectral fit parameters that were used to simulate the RASS to obtain V_{\max} . We take the calculated ages and plot them against the effective temperatures observed at infinity in Fig. 2. The errorbars on the ages correspond to the maximum of the difference in ages obtained due to uncertainties in T_{bb} , N_H (these two parameters are covariant), and the distance. The blackbody temperature T_{bb} is obtained by fitting a blackbody spectrum to that observed from the source. The temperature, thus, corresponds to the color temperature of the object and is an overestimation of the effective temperature T_{eff} due to strong energy dependence of the free-free and bound-free

Table 2. Properties of nearby thermally emitting isolated NSs

Object	P (s)	\dot{P} (10^{-14} s s $^{-1}$)	D (pc)	T_{bb} (eV)	N_H (10^{20} cm $^{-2}$)	F_x	NOB	$t_{stat} \pm \Delta t_{sys}$ (Myr)	$t_{kin/dyn}$ (Myr)
RBS 1223 ¹	10.31 ²	11.20 ²	≥ 525 ³	118 ± 13	0.5 – 2.1	4.5	368^{+32}_{-28}	0.073 ± 0.005	$0.5 - 1$ ²⁵
2XMM J104608.7* ⁴	-	-	2000	117 ± 14	35 ± 11	0.097	1702^{+668}_{-477}	0.089 ± 0.008	
RX J1605.3 + 3249 ⁵	-	-	$325 - 390$ ⁶	$86 - 98$	0.6 – 1.5	1.15	181^{+414}_{-23}	0.23 ± 0.18	$0.45 - 3.5$ ²⁶
RBS 1774 ⁷	9.437 ⁸	4.1 ± 1.8 ⁹	$390 - 430$ ¹⁰	92^{+19}_{-15}	4.6 ± 0.2	8.7	588^{+138}_{-75}	0.28 ± 0.18	
RX J0806.4 – 4123 ¹¹	11.37 ¹²	5.5 ± 3.0 ¹²	240 ± 25 ¹³	78 ± 7	2.5 ± 0.9	2.9	211^{+26}_{-27}	0.41 ± 0.18	
RX J0720.4 – 3125 ¹⁴	8.39 ¹⁵	6.98 ± 0.02 ¹⁵	330^{+170}_{-80} ¹⁶	79 ± 4	1.3 ± 0.3	11.5	278^{+42}_{-35}	0.51 ± 0.18	$0.5 - 1$ ¹⁷
RX J0420.0 – 5022 ¹⁸	3.45 ¹⁹	2.8 ± 0.3 ¹⁹	350 ²⁰	57^{+25}_{-47}	1.7	0.69	713^{+99}_{-89}	0.55 ± 0.18	
RX J1856.5 – 3754 ²¹	7.06 ²²	2.97 ± 0.07 ²²	161^{+18}_{-14} ²³	57 ± 1	1.4 ± 0.1	14.6	604^{+256}_{-115}	0.59 ± 0.18	~ 0.4 ²⁴

F_x (10^{-12} erg cm $^{-2}$ s $^{-1}$) - The absorbed X-ray flux in the ROSAT energy band (0.12 – 2.4 keV).

* 2XMM J104608.7 – 594306 ¹Schwabe et al. (1999) ²Kaplan & van Kerkwijk (2005b) ³Posselt et al. (2007) ⁴Pires et al. (2009)
⁵Motch et al. (1999) ⁶Posselt et al. (2007) ⁷Zampieri et al. (2001) ⁸Zane et al. (2005) ⁹Kaplan & van Kerkwijk (2009b)
¹⁰Posselt et al. (2007) ¹¹Haberl et al. (1998) ¹²Kaplan & van Kerkwijk (2009a) ¹³Motch et al. (2008) ¹⁴Haberl et al. (1997)
¹⁵Kaplan & van Kerkwijk (2005a) ¹⁶Kaplan et al. (2007) ¹⁷Kaplan et al. (2007); Tetzlaff et al. (2011) ¹⁸Haberl et al. (1999)
¹⁹Kaplan & van Kerkwijk (2011) ²⁰Posselt et al. (2007) ²¹Walter et al. (1996) ²²van Kerkwijk & Kaplan (2008)
²³Kaplan et al. (2007) ²⁴Mignani et al. (2013); Tetzlaff et al. (2011); Kaplan et al. (2002); Walter & Lattimer (2002)
²⁵Tetzlaff et al. (2010) ²⁶Tetzlaff et al. (2012)

opacities of the photosphere (see for e.g. Lloyd et al. 2003). The effective temperature is obtained from T_{bb} using a color correction factor $f_c = T_{bb}/T_{eff}$ where $1 \lesssim f_c \lesssim 1.8$ (e.g. Özel 2013). For comparison, we also plot some cooling curves from Yakovlev & Pethick (2004), where the non-superfluid (No SF) model for a $1.3M_\odot$ cannot explain the data. Other model curves show NS cooling behavior if proton superfluidity in the core is taken into account (see Yakovlev & Pethick 2004, for more details on the 1P and 2P models).

3.3 Statistical Ages Vs The True Ages

The ages of isolated NSs have been estimated using different methods, namely from the spin-down law, cooling models, and kinematics. The method we propose in this study to estimate the true ages of these objects has only been applied, in its original form, to estimate the ages of white dwarfs from their cumulative luminosity function in globular cluster (see for e.g. Goldsbury et al. 2012). The method itself is purely a statistical one, for which the underlying assumption is that the objects in the sample follow a Poisson distribution (Felten 1976) with a constant production rate. The important question to ask here is how good of an estimate of the true age is the statistical age. What is the inherent statistical and other errors associated to this method of predicting ages?

3.3.1 Statistical Error

Consider the youngest object, RBS 1223, which is also the hottest among the eight isolated NSs. The kinematic age of RBS 1223 has been found based on its association to possible OB associations and young star clusters to be $\sim 0.5 - 1$ Myr (Tetzlaff et al. 2010), with large uncertainties. The statistical age of RBS 1223 that we find in our study, given that the sample only contains eight such objects, is much smaller $\sim 0.073 \pm 0.005$ Myr, with uncertainties corresponding to systematic errors. The statistical error is of course much larger than the systematic one. Since the discovery of

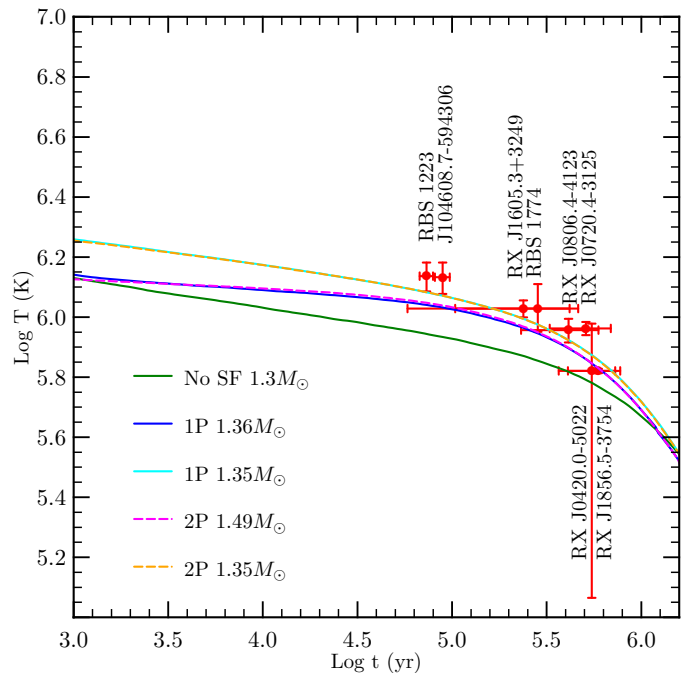


Figure 2. Cooling curve of nearby thermally emitting isolated NSs obtained from model temperatures and statistical ages. The errors in the ages reflect only the systematic error (see Sec. 3.3 for details). We plot sample theoretical cooling curves from Yakovlev & Pethick (2004) for comparison.

an object in a given volume follows Poisson statistics, the relative error scales as $1/\sqrt{N}$ where N is the sample size with ages $t_i \leq t_N$. Therefore, the error in the age of the first object is $\pm t_1$ where t_1 is its statistical age. Likewise, the error in the age of the eighth object is $\pm t_8/\sqrt{8}$. Evidently, one needs a much larger sample to reduce the statistical errors to that comparable to the systematic errors.

3.3.2 Other Errors

The grand assumption made in this work is that all M7 members are essentially the same object but with different ages. Thus, they all follow one cooling curve. That may not be the complete story. These objects may have different masses, surface composition, magnetic fields, and they also may be located with a line of sight with an inhomogeneous HI column density. All of these parameters affect the inferred temperatures and observability of these objects, and hence their statistical ages (see for e.g. the review by Yakovlev & Pethick 2004), as the objects were ordered from hottest to coldest in Eq. 6. Even in a larger sample of isolated NSs, the dominant errors come from systematics and the uncertainty in the progenitor age t_{OB} . In the case of RX J1856.5-3754, the statistical age with its systematic error is $t_{\text{stat}} = 0.59 \pm 0.18$ Myr. Including the statistical error $\Delta t_{\text{stat}} = 0.59/\sqrt{8}$ Myr, since it's the 8th object in the temperature ordered list, and the error due to the uncertainty $\Delta t_{\text{OB}} = 16$ Myr, the total error is $\Delta t_{\text{tot}} = 0.44$ Myr. Systematic errors can be reduced by having better estimates of distances, sensitive surveys that yield accurate surface temperatures, and an improved model of the HI column density. Accurate determination of these parameters is crucial to obtain accurate estimates of V_{max} .

For RX J0720.4-3125, we find that the total error is $\Delta t_{\text{tot}} = 0.41$ Myr. Although we find this object to be younger than RX J1856.5-3754, the large uncertainties in the statistical ages of both objects make it hard to distinguish which is younger. The kinematic ages of these objects tell a different story, where RX J0720.4-3125 is older than RX J1856.5-3754. This discrepancy results from the ordering of objects based on their model temperatures. If both objects are indeed very similar in their mass and surface composition, and have cooled not much differently, then the statistical ages would agree with RX J0720.4-3125 being younger.

4 DISCUSSION

The ages of isolated NSs are primarily important for constraining their inner structure. In addition, they can be useful for accurately determining the birthplace of the object, if its proper motion is known. Similarly, if the SNR-NS association has been made, then the age of the object can reveal its space velocity and the kinematics of the SNR. The knowledge of ages of such objects is also useful for population synthesis models which rely on the spatial and velocity distributions, and the birthrates of NSs. In this study, we propose a statistical method to estimate the true ages of the ROSAT discovered sample comprising the M7. We then use the age estimates along with the derived spectral temperatures to compare the data with some cooling models. The strength of this technique, as discussed earlier, lies in obtaining a larger sample of *coolers*. With only eight objects, the statistical error is indubitably much larger.

We have used the statistical ages and model temperatures of the nearby thermally emitting isolated NSs to derive a cooling curve, under the assumption that all of the objects in the sample are similar in their mass and surface composition, and have also cooled in a similar fashion. Due to the marginal size of the sample, with large statistical errors, it

is not yet meaningful to differentiate between the different cooling models. However, this whole exercise shows that ages of such objects can be inferred statistically and provides another way of determining accurate ages in addition to ages obtained from kinematics and/or spin-down.

The statistics can be improved by locating more of these objects in the disk of the Galaxy. In a recent population synthesis study, Posselt et al. (2010) find that young isolated NSs, that are both hot and bright, with ROSAT count rates below 0.1 cts s^{-1} (the ROSAT bright source catalog had a limiting count rate of 0.05 cts s^{-1}) should be located in OB associations beyond the Gould belt. They also remark on the possibility of finding new isolated cooling NSs by conducting yet another careful search of such objects in the RASS and the XMM-Newton Slew Survey (Esquej et al. 2006). However, they note that ROSAT observations are incapable at locating the isolated sources with sufficient spatial accuracy, such that many optical counterparts can be found in its large positional error circle. On the other hand, although XMM-Newton is much more sensitive, albeit with strong inhomogeneities, and can probe deeper into the Galactic plane, the slew survey only covers 15% of the sky currently. Searching the RASS for new isolated NSs may appear to be a promising avenue (e.g. Turner et al. 2010). What is needed at the moment is another all-sky survey that is able to surpass ROSAT in both sensitivity and positional accuracy. In that regard, the upcoming eROSITA mission (Cappelluti et al. 2011) shows a lot of promise, and its planned launch in 2014 makes it very timely. The X-ray instrument eROSITA will be part of the Russian Spectrum-Roentgen-Gamma (SRG) satellite, equipped with seven Wolter-I telescope modules with an advanced version of the XMM-Newton pnCCD camera at its prime focus. The telescope will operate with an energy range of $0.5 - 10 \text{ keV}$, a field of view (FOV) of 1.03° , an angular resolution of $28''$ averaged over the FOV, and a limiting flux of $\sim 10^{-14} \text{ erg cm}^{-3}$ in the $0.5 - 2 \text{ keV}$ energy range and $\sim 3 \times 10^{-13} \text{ erg cm}^{-3}$ in the $2 - 10 \text{ keV}$ energy range. The all-sky survey will reach sensitivities that are ~ 30 times that of the RASS where the entire sky will be scanned over a period of four years.

5 ACKNOWLEDGEMENTS

We would like to thank the referee for significantly improving the quality of this work. The Natural Sciences and Engineering Research Council of Canada, Canadian Foundation for Innovation and the British Columbia Knowledge Development Fund supported this work. Correspondence and requests for materials should be addressed to J.S.H. (hey1@phas.ubc.ca). This research has made use of NASA's Astrophysics Data System Bibliographic Services

REFERENCES

- An H., Kaspi V. M., Archibald R., Cumming A., 2013, ApJ, 763, 82
- Aschenbach B., Egger R., Trümper J., 1995, Nature, 373, 587
- Avni Y., Bahcall J. N., 1980, ApJ, 235, 694

- Bahcall J. N., Soneira R. M., 1980, *ApJ*, Supplement, 44, 73
- Becker W., ed. 2009, *Neutron Stars and Pulsars Vol. 357 of Astrophysics and Space Science Library*
- Becker W., Pavlov G. G., 2002, *ArXiv Astrophysics e-prints*
- Becker W., Prinz T., Winkler P. F., Petre R., 2012, *ApJ*, 755, 141
- Binney J., Merrifield M., 1998, *Galactic astronomy*. Princeton University Press
- Blazek J. A., Gaensler B. M., Chatterjee S., van der Swaluw E., Camilo F., Stappers B. W., 2006, *ApJ*, 652, 1523
- Cappelluti N., Predehl P., Böhringer H., Brunner H., Brusa M., Burwitz V., Churazov E., Dennerl K., Finoguenov A., Freyberg M., Friedrich P., Hasinger G., Kenziorra E., Kreykenbohm 2011, *Memorie della Societa Astronomica Italiana Supplementi*, 17, 159
- Caswell J. L., Kesteven M. J., Stewart R. T., Milne D. K., Haynes R. F., 1992, *ApJ*, 399, L151
- Clifton T. R., Lyne A. G., 1986, *Nature*, 320, 43
- Colpi M., Geppert U., Page D., 2000, *ApJ*, 529, L29
- Corbel S., Chapuis C., Dame T. M., Durouchoux P., 1999, *ApJ*, 526, L29
- Davies B., Figer D. F., Kudritzki R.-P., Trombly C., Kouveliotou C., Wachter S., 2009, *ApJ*, 707, 844
- Demorest P. B., Pennucci T., Ransom S. M., Roberts M. S. E., Hessels J. W. T., 2010, *Nature*, 467, 1081
- Dermer C. D., Powale G., 2013, *A&A*, 553, A34
- Dewey R. J., Taylor J. H., Weisberg J. M., Stokes G. H., 1985, *ApJ*, 294, L25
- Dib R., Kaspi V. M., Gavriil F. P., 2008, *ApJ*, 673, 1044
- Dib R., Kaspi V. M., Gavriil F. P., 2009, *ApJ*, 702, 614
- Diehl R., Halloin H., Kretschmer K., Lichti G. G., Schönfelder V., Strong A. W., von Kienlin A., Wang W., Jean P., Knödseder J., Roques J.-P., Weidenspointner G., Schanne S., Hartmann D. H., Winkler C., Wunderer C., 2006, *Nature*, 439, 45
- Dodson R. G., McCulloch P. M., Lewis D. R., 2002, *ApJ*, 564, L85
- Esposito P., Burgay M., Possenti A., Turolla R., Zane S., de Luca A., Tiengo A., Israel G. L., Mattana F., Mereghetti S., Bailes M., Romano P., Götz D., Rea N., 2009, *MNRAS*, 399, L44
- Esposito P., Tiengo A., Mereghetti S., Israel G. L., De Luca A., Götz D., Rea N., Turolla R., Zane S., 2009, *ApJ*, 690, L105
- Esquej M. P., Altieri B., Bermejo D., Freyberg M. J., Lazaro V., Read A. M., Saxton R. D., 2006, in A. Wilson ed., *The X-ray Universe 2005 Vol. 604 of ESA Special Publication, The XMM-Newton Slew Survey: Towards the XMMSL1 Catalogue*. p. 965
- Felten J. E., 1976, *ApJ*, 207, 700
- Figer D. F., Najarro F., Geballe T. R., Blum R. D., Kudritzki R. P., 2005, *ApJ*, 622, L49
- Finley J. P., Oegelman H., 1994, *ApJ*, 434, L25
- Foster T., Routledge D., 2003, *ApJ*, 598, 1005
- Frail D. A., Goss W. M., Whiteoak J. B. Z., 1994, *ApJ*, 437, 781
- Gaensler B. M., McClure-Griffiths N. M., Oey M. S., Haverkorn M., Dickey J. M., Green A. J., 2005, *ApJ*, 620, L95
- Gavriil F. P., Kaspi V. M., 2002, *ApJ*, 567, 1067
- Gill R., Heyl J., 2007, *MNRAS*, 381, 52
- Goldreich P., Reisenegger A., 1992, *ApJ*, 395, 250
- Goldsbury R., Heyl J., Richer H. B., Bergeron P., Dotter A., Kalirai J. S., MacDonald J., Rich R. M., Stetson P. B., Tremblay P.-E., Woodley K. A., 2012, *ApJ*, 760, 78
- Gotthelf E. V., Halpern J. P., Alford J., 2013, *ApJ*, 765, 58
- Haberl F., 2007, *Ap&SS*, 308, 181
- Haberl F., Motch C., Buckley D. A. H., Zickgraf F.-J., Pietsch W., 1997, *A&A*, 326, 662
- Haberl F., Motch C., Pietsch W., 1998, *Astronomische Nachrichten*, 319, 97
- Haberl F., Pietsch W., Motch C., 1999, *A&A*, 351, L53
- Halpern J. P., 2011, *ApJ*, 736, L3
- Halpern J. P., Gotthelf E. V., 2010a, *ApJ*, 709, 436
- Halpern J. P., Gotthelf E. V., 2010b, *ApJ*, 710, 941
- Hartwick F. D. A., Schade D., 1990, *ARA&A*, 28, 437
- Hester J. J., 2008, *ARA&A*, 46, 127
- Heyl J. S., Hernquist L., 1998, *MNRAS*, 297, L69
- Heyl J. S., Kulkarni S. R., 1998, *ApJ*, 506, L61
- Hobbs G., Lyne A. G., Kramer M., Martin C. E., Jordan C., 2004, *MNRAS*, 353, 1311
- Huchra J., Sargent W. L. W., 1973, *ApJ*, 186, 433
- Hulse R. A., Taylor J. H., 1975, *ApJ*, 201, L55
- Hünsch M., Schmitt J. H. M. M., Sterzik M. F., Voges W., 1999, *A&AS*, 135, 319
- Johnston S., Lyne A. G., Manchester R. N., Kniffen D. A., D'Amico N., Lim J., Ashworth M., 1992, *MNRAS*, 255, 401
- Kaplan D. L., Kulkarni S. R., van Kerkwijk M. H., Marshall H. L., 2002, *ApJ*, 570, L79
- Kaplan D. L., van Kerkwijk M. H., 2005a, *ApJ*, 628, L45
- Kaplan D. L., van Kerkwijk M. H., 2005b, *ApJ*, 635, L65
- Kaplan D. L., van Kerkwijk M. H., 2009a, *ApJ*, 705, 798
- Kaplan D. L., van Kerkwijk M. H., 2009b, *ApJ*, 692, L62
- Kaplan D. L., van Kerkwijk M. H., 2011, *ApJ*, 740, L30
- Kaplan D. L., van Kerkwijk M. H., Anderson J., 2002, *ApJ*, 571, 447
- Kaplan D. L., van Kerkwijk M. H., Anderson J., 2007, *ApJ*, 660, 1428
- Kaspi V. M., Manchester R. N., Siegman B., Johnston S., Lyne A. G., 1994, *ApJ*, 422, L83
- Kovalenko A. V., 1989, *Soviet Astronomy Letters*, 15, 144
- Large M. I., Vaughan A. E., Mills B. Y., 1968, *Nature*, 220, 340
- Lloyd D. A., Hernquist L., Heyl J. S., 2003, *ApJ*, 593, 1024
- Lyne A. G., Graham-Smith F., 2006, *Pulsar Astronomy*. Cambridge University Press
- Lyne A. G., Pritchard R. S., Graham-Smith F., Camilo F., 1996, *Nature*, 381, 497
- Manchester R. N., Damico N., Tuohy I. R., 1985, *MNRAS*, 212, 975
- Manchester R. N., Hobbs G. B., Teoh A., Hobbs M., 2005, *VizieR Online Data Catalog*, 7245, 0
- Manchester R. N., Tuohy I. R., Damico N., 1982, *ApJ*, 262, L31
- Mereghetti S., 2011, in Torres D. F., Rea N., eds, *High-Energy Emission from Pulsars and their Systems X-ray emission from isolated neutron stars*. p. 345
- Mereghetti S., Esposito P., Tiengo A., Zane S., Turolla R., Stella L., Israel G. L., Götz D., Feroci M., 2006, *ApJ*, 653, 1423
- Mignani R. P., Vande Putte D., Cropper M., Turolla R., Zane S., Pellizza L. J., Bignone L. A., Sartore N., Treves

- A., 2013, *MNRAS*, 429, 3517
- Motch C., Haberl F., Zickgraf F.-J., Hasinger G., Schwöpe A. D., 1999, *A&A*, 351, 177
- Motch C., Pires A. M., Haberl F., Schwöpe A., Zavlin V. E., 2008, in C. Bassa, Z. Wang, A. Cumming, & V. M. Kaspi ed., *40 Years of Pulsars: Millisecond Pulsars, Magnetars and More* Vol. 983 of American Institute of Physics Conference Series, Proper motions of ROSAT discovered isolated neutron stars measured with Chandra: First X-ray measurement of the large proper motion of RX J1308.6+2127/RBS 1223. pp 354–356
- Motch C., Pires A. M., Haberl F., Schwöpe A., Zavlin V. E., 2009, *A&A*, 497, 423
- Motch C., Sekiguchi K., Haberl F., Zavlin V. E., Schwöpe A., Pakull M. W., 2005, *A&A*, 429, 257
- Muno M. P., Clark J. S., Crowther P. A., Dougherty S. M., de Grijs R., Law C., McMillan S. L. W., Morris M. R., Negueruela I., Pooley D., Portegies Zwart S., Yusef-Zadeh F., 2006, *ApJ*, 636, L41
- Nakagawa Y. E., Mihara T., Yoshida A., Yamaoka K., Sugita S., Murakami T., Yonetoku D., Suzuki M., Nakajima M., Tashiro M. S., Nakazawa K., 2009, *PASJ*, 61, 387
- Nugent R. L., 1998, *PASP*, 110, 831
- Özel F., 2013, *Reports on Progress in Physics*, 76, 016901
- Page D., Geppert U., Weber F., 2006, *Nuclear Physics A*, 777, 497
- Park S., Hughes J. P., Slane P. O., Burrows D. N., Lee J.-J., Mori K., 2012, *ApJ*, 748, 117
- Park S., Hughes J. P., Slane P. O., Mori K., Burrows D. N., 2010, *ApJ*, 710, 948
- Pires A. M., Motch C., Janot-Pacheco E., 2009, *A&A*, 504, 185
- Pons J. A., Miralles J. A., Geppert U., 2009, *A&A*, 496, 207
- Posselt B., Popov S. B., Haberl F., Trümper J., Turolla R., Neuhäuser R., 2007, *Ap&SS*, 308, 171
- Posselt B., Popov S. B., Haberl F., Trümper J., Turolla R., Neuhäuser R., Boldin P. A., 2010, *A&A*, 512, C2
- Rutledge R. E., Fox D. B., Shevchuk A. H., 2008, *ApJ*, 672, 1137
- Sasaki M., Plucinsky P. P., Gaetz T. J., Bocchino F., 2013, *A&A*, 552, A45
- Sato T., Bamba A., Nakamura R., Ishida M., 2010, *PASJ*, 62, L33
- Sawada M., Koyama K., 2012, *PASJ*, 64, 81
- Schaab C., Weber F., Weigel M. K., Glendenning N. K., 1996, *Nuclear Physics A*, 605, 531
- Schmidt M., 1968, *ApJ*, 151, 393
- Schwöpe A. D., Hasinger G., Schwarz R., Haberl F., Schmidt M., 1999, *A&A*, 341, L51
- Seward F. D., Harnden Jr. F. R., 1982, *ApJ*, 256, L45
- Seward F. D., Harnden Jr. F. R., Helfand D. J., 1984, *ApJ*, 287, L19
- Seward F. D., Harnden Jr. F. R., Murdin P., Clark D. H., 1983, *ApJ*, 267, 698
- Shapiro S. L., Teukolsky S. A., 1983, *Black holes, white dwarfs, and neutron stars: The physics of compact objects*
- Smartt S. J., 2009, *ARA&A*, 47, 63
- Sun M., Seward F. D., Smith R. K., Slane P. O., 2004, *ApJ*, 605, 742
- Tendulkar S. P., Cameron P. B., Kulkarni S. R., 2012, *ApJ*, 761, 76
- Tetzlaff N., Eisenbeiss T., Neuhäuser R., Hohle M. M., 2011, *MNRAS*, 417, 617
- Tetzlaff N., Neuhäuser R., Hohle M. M., Maciejewski G., 2010, *MNRAS*, 402, 2369
- Tetzlaff N., Schmidt J. G., Hohle M. M., Neuhäuser R., 2012, *PASA*, 29, 98
- Tiengo A., Esposito P., Mereghetti S., Israel G. L., Stella L., Turolla R., Zane S., Rea N., Götz D., Feroci M., 2009, *MNRAS*, 399, L74
- Torra J., Fernández D., Figueras F., 2000, *A&A*, 359, 82
- Turner M. L., Rutledge R. E., Letcavage R., Shevchuk A. S. H., Fox D. B., 2010, *ApJ*, 714, 1424
- van Kerkwijk M. H., Kaplan D. L., 2008, *ApJ*, 673, L163
- Vasisht G., Gotthelf E. V., 1997, *ApJ*, 486, L129
- Vasisht G., Kulkarni S. R., Anderson S. B., Hamilton T. T., Kawai N., 1997, *ApJ*, 476, L43
- Vink J., 2004, *ApJ*, 604, 693
- Voges W., Aschenbach B., Boller T., Bräuninger H., Briel U., Burkert W., Dennerl K., Englhauser J., Gruber R., Haberl F., Hartner G., 1999, *A&A*, 349, 389
- Walter F. M., Lattimer J. M., 2002, *ApJ*, 576, L145
- Walter F. M., Wolk S. J., Neuhäuser R., 1996, *Nature*, 379, 233
- Weisskopf M. C., Elsner R. F., Darbro W., Leahy D., Narayan S., Harnden F. R., Seward F. D., Sutherland P. G., Grindlay J. E., 1983, *ApJ*, 267, 711
- Winkler P. F., Kirshner R. P., 1985, *ApJ*, 299, 981
- Wolszczan A., Cordes J. M., Dewey R. J., 1991, *ApJ*, 372, L99
- Yakovlev D. G., Kaminker A. D., Gnedin O. Y., Haensel P., 2001, *Phys. Rep.*, 354, 1
- Yakovlev D. G., Pethick C. J., 2004, *ARA&A*, 42, 169
- Yar-Uyaniker A., Uyaniker B., Kothes R., 2004, *ApJ*, 616, 247
- Yuan J. P., Wang N., Manchester R. N., Liu Z. Y., 2010, *MNRAS*, 404, 289
- Zampieri L., Campana S., Turolla R., Chierigato M., Falomo R., Fugazza D., Moretti A., Treves A., 2001, *A&A*, 378, L5
- Zane S., Cropper M., Turolla R., Zampieri L., Chierigato M., Drake J. J., Treves A., 2005, *ApJ*, 627, 397
- Zane S., Haberl F., Israel G. L., Pellizzoni A., Burgay M., Mignani R. P., Turolla R., Possenti A., Esposito P., Champion D., Eatough R. P., Barr E., Kramer M., 2011, *MNRAS*, 410, 2428